

# Coexistence of $s$ -wave Superconductivity and Antiferromagnetism

M. Feldbacher<sup>1</sup>, F.F. Assaad<sup>1,2</sup>, F. Hébert<sup>3</sup>, and G. G. Batrouni<sup>4</sup>

1. Institut für Theoretische Physik III, Universität Stuttgart,  
Pfaffenwaldring 57, D-70550 Stuttgart, Germany, Germany.

2. Max Planck institute for solid state research, Heisenbergstr. 1, D-70569, Stuttgart, Germany.

3. Theoretische Physik, Universität des Saarlandes, 66041 Saarbrücken, Germany.

4. Institut Non-Linéaire de Nice, Université de Nice-Sophia Antipolis,  
1361 route des Lucioles, 06560 Valbonne, France.

We study the phase diagram of a new model that exhibits a first order transition between  $s$ -wave superconducting and antiferromagnetic phases. The model, a generalized Hubbard model augmented with competing spin-spin and pair-pair interactions, was investigated using the projector Quantum Monte Carlo method. Upon varying the Hubbard  $U$  from attractive to repulsive we find a first order phase transition between superconducting and antiferromagnetic states.

PACS numbers: 71.27.+a, 71.10.-w, 71.10.Fd

Experimental phase diagrams with superconducting and magnetic phases in close proximity continue to fascinate since the broken symmetry states are incompatible. In particular, a canonical two-dimensional example is the layered organic superconductor  $\kappa$ -(BEDT-TTF)<sub>2</sub>Cu[N(CN)<sub>2</sub>]Cl which shows a first order transition between antiferromagnetic (AF) insulating and superconducting (SC) phases upon varying the pressure.[1] Debate continues about the nature of the superconducting state. Kanoda et al. argue that NMR data are consistent with an unconventional superconducting gap with nodal lines.[2] Conversely, many experimental studies are rather consistent with  $s$ -wave, phonon mediated superconductivity. In particular, Kini et al. could demonstrate a BCS-like mass isotope effect in  $\kappa$ -S.[3] The same material exhibits a strong superconductivity induced (acoustic) phonon renormalization. [4] Nodes in the pair order parameter are also incompatible with specific heat measurements.[5]

In order to model the scenario of a phase transition between an AF and an  $s$ -wave SC on a half-filled two dimensional lattice we add to the standard Hubbard model a pair hopping term:

$$H = -t \sum_{\langle \vec{i}, \vec{j} \rangle, \sigma} \left( c_{\vec{i}, \sigma}^\dagger c_{\vec{j}, \sigma} + H.c. \right) + U \sum_{\vec{i}} n_{\vec{i}, \uparrow} n_{\vec{i}, \downarrow} \quad (1)$$

$$- t_p \left( \sum_{\sigma} c_{\vec{i}, \sigma}^\dagger c_{\vec{j}, \sigma} + H.c. \right)^2 - 4V \sum_{\langle \vec{i}, \vec{j} \rangle} \eta_{\vec{i}}^z \eta_{\vec{j}}^z$$

where  $\vec{i}$  labels the sites of a square lattice and the first sum runs over nearest neighbor bonds. The fermionic spin is given by  $\vec{S}_{\vec{i}} = \frac{1}{2} \sum_{s,t} c_{\vec{i}, s}^\dagger \vec{\sigma}_{s,t} c_{\vec{i}, t}$  and  $\vec{\sigma}$  denotes the Pauli matrices. For a dimer the pair hopping term arises exactly when we assume a Su-Schrieffer-Heeger electron-phonon interaction [6] and integrate out the phonon in the antiadiabatic limit. We introduce a particle-hole transformation  $\mathcal{P}$  with properties  $\mathcal{P} c_{\vec{i}, \uparrow} \mathcal{P} = c_{\vec{i}, \uparrow}$ ,

$\mathcal{P} c_{\vec{i}, \downarrow} \mathcal{P} = (-1)^{\vec{i}} c_{\vec{i}, \downarrow}^\dagger$  and  $\mathcal{P}^2 = \mathcal{P}$ . Next we define the pairing operators as [7]  $\vec{\eta}_{\vec{i}} = \mathcal{P} \vec{S}_{\vec{i}} \mathcal{P}$ , the pair creation operator  $\eta_{\vec{i}}^\dagger = (-1)^{\vec{i}} c_{\vec{i}, \uparrow}^\dagger c_{\vec{i}, \downarrow}^\dagger$  and  $\eta_{\vec{i}}^z = (n_{\vec{i}, \uparrow} + n_{\vec{i}, \downarrow} - 1)/2$  is the total charge. The pair hopping term may be recast [8] as  $-\left( \sum_{\sigma} c_{\vec{i}, \sigma}^\dagger c_{\vec{j}, \sigma} + H.c. \right)^2 = 4 \left( \vec{S}_{\vec{i}} \vec{S}_{\vec{j}} + \vec{\eta}_{\vec{i}} \vec{\eta}_{\vec{j}} - \frac{1}{4} \right)$ . For the simulations, we have used the projector auxiliary field QMC algorithm which is well suited for the study of ground state properties [8]. Simulations do not suffer from a sign problem in the region of attractive  $U < 0$  with the additional constraint  $U \leq -8|V|$ . This is the shaded region in Fig. 1. Using particle-hole symmetry the region of repulsive  $U$  at  $V = 0$  is also accessible.

Two  $SU(2)_{S, \eta}$  symmetry groups are generated by the spin algebra  $[S_{\vec{i}}^+, S_{\vec{j}}^-] = 2\delta_{\vec{i}, \vec{j}} S_{\vec{i}}^z$  and its particle-hole equivalent for the  $\eta$  operators. Note that the commutator  $[\vec{S}_{\vec{i}}, \vec{\eta}_{\vec{i}}] = 0$  because  $S_{\vec{i}}^\alpha \eta_{\vec{i}}^\beta = 0$ . The hopping terms  $H_t$  and  $H_p$  are known to be invariant under spin rotation and also commute with the discrete symmetry  $\mathcal{P}$ . This in turn implies that  $\vec{\eta}_{\vec{i}} = \mathcal{P} \vec{S}_{\vec{i}} \mathcal{P}$  also commutes with both hopping terms. The symmetries of the Hubbard term become apparent after putting it into the form

$$H_U = U/3 \sum_{\vec{i}} \left[ (\vec{\eta}_{\vec{i}})^2 - (\vec{S}_{\vec{i}})^2 \right]. \quad (2)$$

We can read off the  $SU(2)_S \otimes SU(2)_\eta$  symmetry and observe that the Hubbard term changes sign under  $\mathcal{P}$  transformation. [7] In Fig. 1 the various symmetries for different parameter regions are displayed. Bars denote symmetries which we numerically find to be spontaneously broken in the thermodynamic limit. The point  $U = V = 0$  has the full symmetry:  $SU(2)_S \otimes SU(2)_\eta \otimes Z_{2, PH}$  where  $Z_{2, PH}$  denotes the discrete particle-hole symmetry. Here two scenarios are possible: i) Long range order for both AF and SC correlations since one implies the other through  $Z_{2, PH}$  symmetry or ii) The competition between the two broken symmetry states leads to a disordered

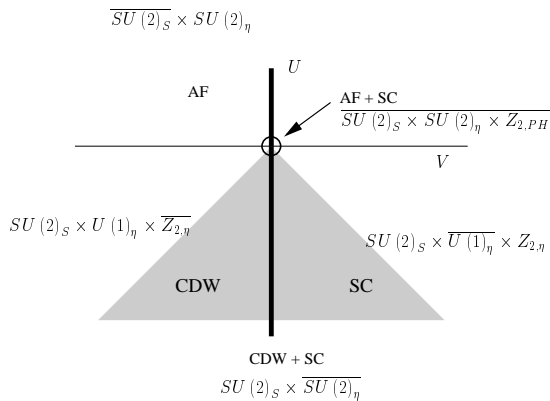


FIG. 1: The phase diagram for the full Hamiltonian. The shaded region indicates the parameters accessible to sign-free simulations. For every region in the phase diagram the full symmetry of the Hamiltonian is indicated. Broken symmetries are marked by bars.

state. We find that the system realizes the first possibility of coexistence of s-wave SC and AF. Switching on  $U$  breaks the particle-hole symmetry whereas  $V$  reduces the  $SU(2)_\eta \rightarrow U(1) \otimes Z_{2,\eta}$ .

In the following, we will first discuss the phase transition at constant negative  $U$  as a function of  $V$  and then turn our attention to the phase transition at  $V = 0$  and varying  $U$ .

In the  $U \rightarrow -\infty$  limit the model is equivalent to hard-core bosons with repulsive nearest neighbor interactions. At half-filling this system experiences a transition from SC to charge-density wave states (CDW) going across  $V = 0$ . [9] The transition point is marked by the higher symmetry  $SU(2)_\eta$  and broken symmetry states may be labeled according to the direction of the magnetization. Therefore it is possible to find broken symmetry states which show a coexistence of CDW and SC order parameters. One can view this as a consequence of merging the Ising and the  $U(1)$  symmetries into a continuous group.

The same behavior is still present for finite attractive  $U$ . In particular our simulations show (see Figs. 3b and 6b) that single particle excitations are always gapped so we can argue that the system still renormalizes to the bosonic model. As we will see, crossing the  $V = 0$  line at  $T = 0$ , we observe a divergence of the correlation length (Fig. 2) which points to a second order phase transition. Furthermore, we find no sign of a discontinuity in the first derivative of the free energy  $(1/N)\partial F/\partial V = -2\langle n_i n_{i+\vec{x}} \rangle$  (see Fig. 3a). At the same time we observe a jump for the CDW and SC order parameters at  $V = 0$ . To understand this transition, we split it up into three parts: a)  $V \rightarrow 0^-$ , b)  $V = 0^- \rightarrow 0^+$  and c)  $V \rightarrow 0^+$ . Part b) is responsible for the jump in the order parameters. Let us introduce

the two limiting ground states via

$$\Psi_{\text{Ising}} = \lim_{V \rightarrow 0^-} \lim_{N \rightarrow \infty} \Psi(V) \quad (3)$$

$$\Psi_{\text{XY}} = \lim_{V \rightarrow 0^+} \lim_{N \rightarrow \infty} \Psi(V). \quad (4)$$

The ground state in the Ising regime  $\Psi_{\text{Ising}}$  has CDW order and the SC order parameter is zero. Jumping to positive  $V$  and  $\Psi_{\text{XY}}$  the situation reverses. Thus the observed jump in the order parameters is the simple consequence of forcing the transition from one broken symmetry state to the other:  $\Psi_{\text{Ising}} \rightarrow \Psi_{\text{XY}}$ . Next we look at the critical behavior as we approach the phase transition from either side. Linear spin wave theory (LSWT) predicts for both transitions a) and c) the same square root divergence for the respective transverse correlation function. In case c) the equal time transverse correlation function is  $\langle n_{\vec{Q}} n_{-\vec{Q}} \rangle$  where  $n_{\vec{Q}} = (1/\sqrt{N}) \sum_{\vec{r}} e^{i\vec{Q}\vec{r}} n_{\vec{r}}$ ,  $n_{\vec{r}} = n_{\vec{r},\uparrow} + n_{\vec{r},\downarrow}$  and  $\vec{Q} = (\pi, \pi)$ . According to LSWT this density-density correlation diverges like  $\langle n_{\vec{Q}} n_{-\vec{Q}} \rangle = 8S/\sqrt{V/t_p}$  as  $V \rightarrow 0^+$ . The real part of the uniform susceptibility

$$\chi'_{n,n}(\vec{k} = \vec{Q}, \omega = 0) = \int_0^\infty d\tau \langle n_{\vec{Q}} n_{-\vec{Q}} \rangle(\tau) \quad (5)$$

picks up the inverse of the gap  $\Delta = 8\sqrt{2Vt_p}$  and in LSWT diverges like  $\chi'_{n,n}(\vec{Q}, 0) = \sqrt{1/2S/V}$ . Asymptotically the correlation function  $\langle n_{\vec{r}} n_0 \rangle(\tau)$  decays exponentially in space and time thus the integrated correlation functions are proportional to the correlation length and gap

$$\langle n_{\vec{Q}} n_{-\vec{Q}} \rangle \propto \xi^2 \quad (6)$$

$$\chi'_{n,n}(\vec{k} = \vec{Q}, \omega = 0) \propto \xi^2 \Delta^{-1}. \quad (7)$$

Data for both  $\chi'_{n,n}(\vec{Q}, 0)$  and  $\langle n_{\vec{Q}}^z n_{-\vec{Q}}^z \rangle(\tau = 0)$  are shown in Fig. 2 where the dotted line plots the LSWT result multiplied with a single constant to account for the reduced moment.

The ordered state in the XY regime has one Goldstone mode and the transverse correlations  $\langle n_{\vec{Q}} n_{-\vec{Q}} \rangle$  are gapped. Approaching the critical point the gap closes and the  $\langle n_{\vec{Q}} n_{-\vec{Q}} \rangle$  correlation length diverges. Thus critical behavior reflects the softening of the observed mode which turns into a Goldstone mode at the point with higher symmetry. Ultimately it is the softening of the transverse mode which is responsible for the observed critical behavior.

Following the  $V = 0$  line as  $U \rightarrow 0$  the bosonic LRO decreases only slightly leading to a finite limit at  $U = 0^+$  which is shown in Fig. 4. Crossing the  $U = 0$  point we encounter again a phase transition which is linked to a point with higher symmetry: the discrete particle-hole symmetry. Using the  $Z_{2,PH}$  symmetry, one can map this bosonic LRO to an equivalent spin LRO for the repulsive

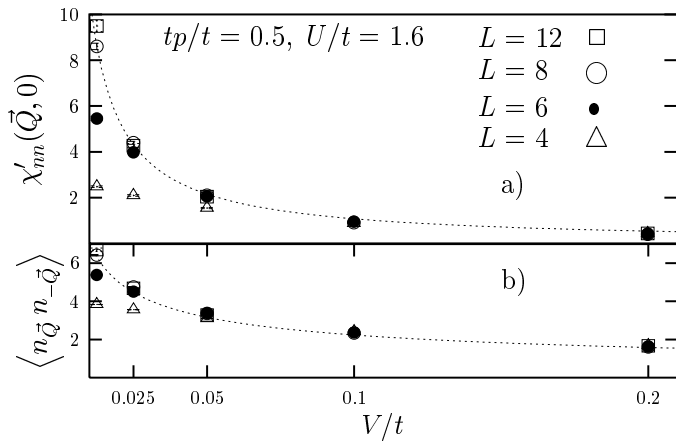


FIG. 2: a) Uniform susceptibility  $\chi'_{n,n}(\vec{Q}, 0) \propto \xi^2 \Delta^{-1}$  b)  $\langle n_{\vec{Q}} n_{-\vec{Q}} \rangle \propto \xi^2$ . The dotted line is proportional to results from LSWT.

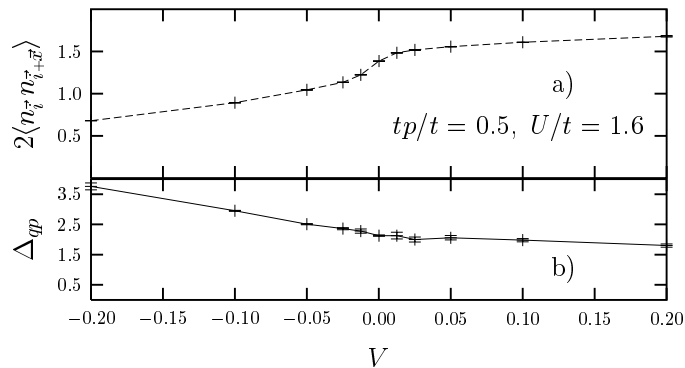


FIG. 3: a) Density-density correlations  $2\langle n_i n_{i+x} \rangle = -1/N(\partial F/\partial V)$  where  $n_i = n_{i,\uparrow} + n_{i,\downarrow}$ . The derivative of the free energy is continuous. b) The quasi-particle gap  $\Delta_{qp}$  was obtained by fitting the tail of the imaginary time correlation function  $G(\tau)$ .

$U$  case at  $V = 0$ . Precisely at  $U = 0$  particle hole symmetry implies that bose correlation functions are equal to their spin counterparts

$$\langle S_{\vec{k}+\vec{Q}}^\alpha S_{-\vec{k}-\vec{Q}}^\alpha \rangle = \langle \eta_{\vec{k}}^\alpha \eta_{-\vec{k}}^\alpha \rangle. \quad (8)$$

This explains a jump by a factor two for the density-density correlations as one moves from the symmetric point to a finite  $U$  which is visible in Fig. 4. The emergence of a Goldstone mode above was associated with the critical behavior of the phase transition. As we are now approaching the  $U = 0$  point the only continuous symmetry available which is not associated with the bosonic LRO is the spin symmetry. In Fig. 5 we compute the correlation length for  $\langle S_{\vec{Q}}^z S_{-\vec{Q}}^z \rangle$ . This quantity shows no sign of divergence at the phase transition. Contrary to what happened in the SC to CDW transition we may classify

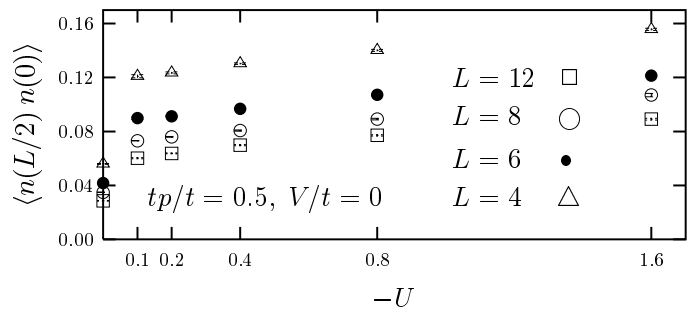


FIG. 4: The density-density correlation function  $1/N \langle n(L/2)n(0) \rangle$  at maximum separation  $(L/2, L/2)$ . The correlation function jumps by a factor two once a finite Hubbard  $U$  term breaks the  $Z_{2,PH}$  symmetry.

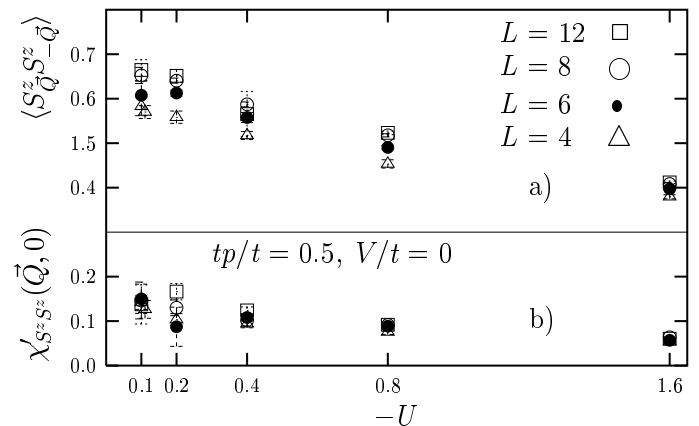


FIG. 5: Values for the uniform susceptibility  $\chi'_{S^z, S^z}(\vec{k} = \vec{Q}, \omega = 0) \propto \xi^2 \xi^z$  (lower curve) are well below the correlation function  $\langle S_{\vec{k}}^z S_{-\vec{k}}^z \rangle(\vec{k} = \vec{Q}) \propto \xi^2$

this transition as a first order level crossing transition. From Fig. 6 we equally see that the derivative of the free energy with respect to  $U$  is discontinuous. The free energy as a function of double occupancy has a plateau which marks a region of phase coexistence.

For the point  $U = V = 0$  we find coexistence of the spin and pair order parameters. After finite size extrapolation the results of Fig. 7 are consistent with a finite value of the magnetization  $m_s$  up to weak coupling ( $t_p/t \ll 1$ ). At the same time the superconducting order parameter  $\Delta$  is also nonzero and the measured value  $\Delta = \sqrt{2}m_s$  agrees with Eq. 8. The observed coexistence of AF and SC order is due to the special particle-hole symmetry  $Z_{2,PH}$  at the point  $U = 0$  which renders the energies of both the AF and SC states degenerate.

In order to understand how the  $SU(2)_S \otimes SU(2)_\eta$  symmetries are spontaneously broken we also need to discuss whether the discrete particle-hole symmetry is broken and how this affects the spontaneous breaking of the continuous symmetries. We introduce the following pseudo-

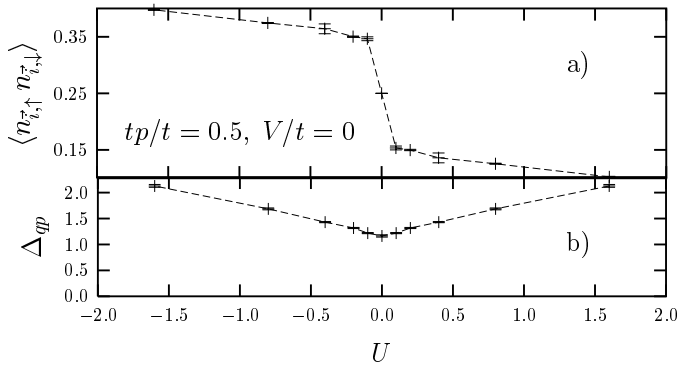


FIG. 6: a) The "Hubbard" correlation  $\langle n_{\uparrow} n_{\downarrow} \rangle = 1/N(\partial F/\partial U)$  has a jump at the transition point  $U = 0$ . The first order transition is signaled by a discontinuity of the first derivative of the free energy. b) The quasi-particle gap  $\Delta_{qp}$ .

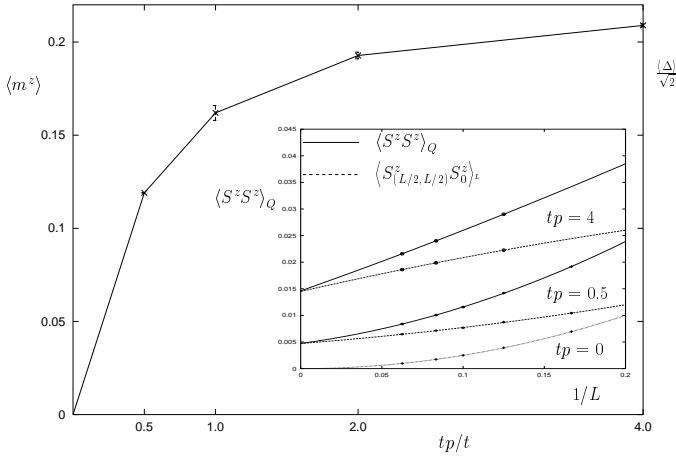


FIG. 7: The staggered moment  $m_s$  which coexists with the superconducting order parameter  $\Delta = m_s \sqrt{2}$  plotted as a function of  $t_p$  ( $U/t = V/t = 0$ ). The inset shows finite size extrapolation for  $t_p = 4$  and  $t_p = 0.5$ .

spin order parameter

$$\mathcal{S}_i^z = ((2S_i^z)^2 - (2\eta_i^z)^2) \begin{cases} +1 : |\uparrow\rangle, |\downarrow\rangle \\ -1 : |\uparrow\downarrow\rangle, |0\rangle \end{cases}, \quad (9)$$

$$\langle \mathcal{S} \rangle = \langle \mathcal{PSP} \rangle = -\langle \mathcal{S} \rangle \quad (10)$$

which has to be zero as long as the  $Z_{2,PH}$  symmetry is not broken as assumed in Eq. (10). A positive (negative) value for  $\langle \mathcal{S} \rangle$  indicates a majority of spins (pairs) in the system. Plotting the uniform correlations  $1/N \langle \mathcal{S}_{\vec{k}} \mathcal{S}_{\vec{k}} \rangle (\vec{k} = 0)$  as a function of temperature, one sees in Fig. 8 that below a temperature  $T_c \sim 1.8t$  particle-hole symmetry is indeed broken. Hence below  $T_c$  and in the thermodynamic limit the  $Z_{2,PH}$  particle-hole symmetry is broken and depending on the orientation of the pseudo-spin,  $\mathcal{S}_i^z$ , the SC or AF ground state will be chosen.

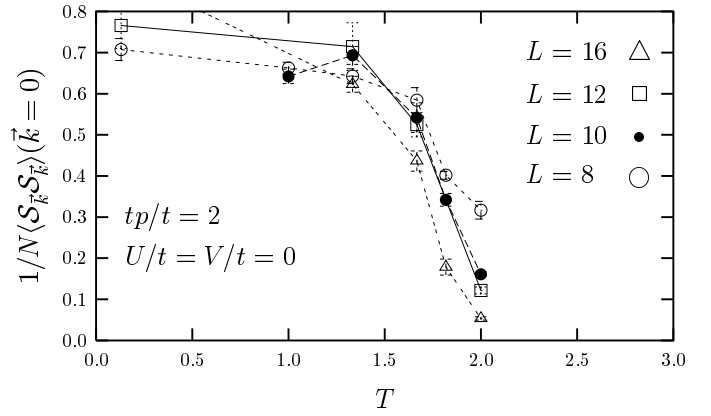


FIG. 8: The  $1/N \langle \mathcal{S}_{\vec{k}} \mathcal{S}_{\vec{k}} \rangle (\vec{k} = 0)$  correlations show that at least up to  $T \leq 1.8t$  particle-hole symmetry is broken.

In conclusion we have considered a model with competing interactions. The main ingredients in the model are on the one hand the Heisenberg and Hubbard terms which lead to a localization of single electrons thereby producing antiferromagnetic insulating states and on the other hand, pair hopping and nearest neighbor attractive terms which lead to on-site s-wave superconducting states. Based on the symmetries of the model as well as quantum Monte Carlo simulations we have shown that the model has a variety of phase transitions. In particular we have found a first order phase transition between an s-wave superconducting state and antiferromagnetic Mott insulator at a high symmetry point ( $U = V = 0$ ) where the two phases coexist.

We wish to thank the HLR-Stuttgart for generous allocation of computer time, the DFG for financial support (grant numbers AS 120/1-3, AS 120/1-1) as well as a joint Franco-German cooperative grant (PROCOPE).

- 
- [1] S. Lefebvre, P. Wzietek, S. Brown, C. Bourbonnais, D. Jérôme, C. Mézière, M. Fourmigué and P. Batail, Phys. Rev. Lett. **85**, 5420 (2000)
  - [2] K. Kanoda, K. Miyagawa, A. Kawamoto, and Y. Nakazawa, Phys. Rev. B **54**, 76 (1996).
  - [3] A. M. Kini *et al.*, Physica C **264**, 81, (1996).
  - [4] L. Pintschovius *et al.*, Europhys. Lett. **37**, 627 (1997)
  - [5] J. Müller, M. Lang, R. Helfrich, F. Steglich, and T. Sasaki, Phys. Rev. B **65**, 140509 (2002).
  - [6] W. P. Su, J. R. Schrieffer and A. J. Heeger, Phys. Rev. B **22**, 2099 (1980)
  - [7] C. N. Yang and S. C. Zhang, Mod. Phys. Lett. **B 4**, 759 (1990)
  - [8] S. Capponi and F. F. Assaad, Phys. Rev. B **63**, 155114 (2001)
  - [9] F. Hébert *et al.*, Phys. Rev. B **65**, 014513 (2002)